

Figure 1. (A) Proton NMR spectrum (6.0–14.5 ppm) of the G·A 12-mer duplex in 0.1 M NaCl, 10 mM phosphate, and 92% H₂O, pH 8.3 at 0 °C. (B) One-dimensional NOE difference spectrum following 0.4-s saturation of the 13.42 ppm imino proton of G3 (designated by arrow).

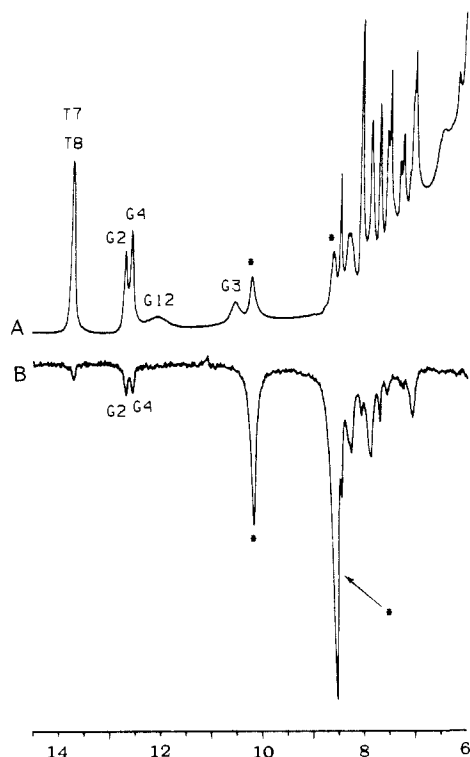


Figure 2. (A) Proton NMR spectrum (6.0–14.5 ppm) of the G·A 12-mer duplex in 0.1 M NaCl, 10 mM phosphate, and 92% H₂O, pH 4.3 at 0 °C. (B) One-dimensional NOE difference spectrum following 0.4-s saturation of 8.59 ppm amino proton (designated by arrow).

NMR spectra were recorded on 2.5 mM dodecanucleotide duplexes in 0.1 M NaCl, 10 mM phosphate, and 0.1 mM EDTA, aqueous solution. The pH values quoted in D₂O solution are uncorrected pH meter readings.

Proton and phosphorus spectra were recorded on Bruker AM 400 and AM 300 spectrometers, respectively. Phase-sensitive two-dimensional NOESY and COSY data sets were recorded under conditions described previously²⁰ and processed with the Dennis Hare FTNMR software.

Results

Exchangeable Proton Spectra. The exchangeable proton spectra (6–14.5 ppm) of the G·A 12-mer duplex in H₂O buffer, 0 °C,

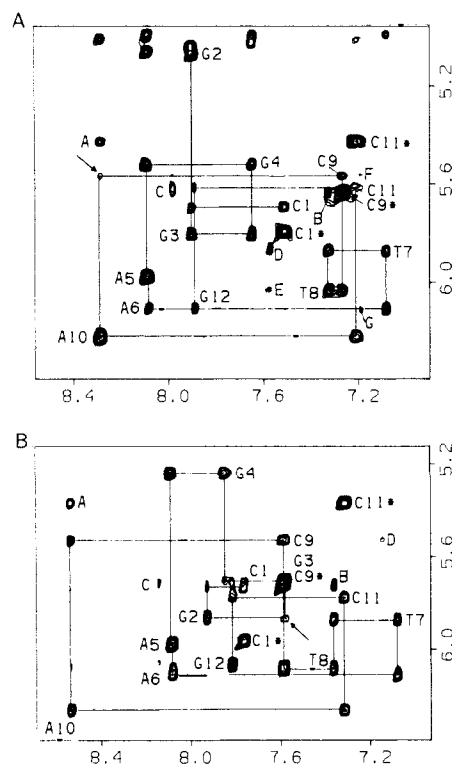


Figure 3. Expanded contour plots of the phase-sensitive NOESY (250-ms mixing time) spectra of the G·A 12-mer duplex in 0.1 M NaCl, 10 mM phosphate, and D₂O, 25 °C at (A) pH 6.8 and (B) pH 4.2. This region establishes distance connectivities between the base protons (7.0–8.6 ppm) and the sugar H1' and cytidine H5 protons (5.0–6.4 ppm). The cytidines H5–H6 cross peaks are designated by asterisks and labeled cross peaks are discussed in the text. The lines follow connectivities between adjacent base protons through their intervening sugar H1' protons.

exhibit dramatically different chemical shifts indicative of distinct neutral pH (pH 6.5–8.5) (Figure 1A) and low pH (pH 4.0–5.5) (Figure 2A) conformations. We also detect resonances from both conformations at intermediate pH values characteristic of slow exchange between structures on the NMR time scale.

The imino protons in the neutral pH conformation at 0 °C have been assigned from one-dimensional NOE measurements and are listed above the resonances in Figure 1A. The imino proton of G3 at the G3·A10 mismatch site is broad at 0 °C in the neutral pH spectrum but narrows on raising the pH and temperature. We detect a NOE between the 13.42 ppm imino proton of G3 and the 7.95 ppm H2 proton of A10 for the G3·A10 mismatch in the G·A 12-mer at pH 8.3 and 0 °C (figure 1B).

The imino protons of the G·A 12-mer acidic pH conformation at 0 °C (Figure 2A) have been assigned from one-dimensional NOE measurements, as well as saturation transfer experiments on a 1:1 mixture of neutral and acidic pH conformations at pH 5.8. Thus, saturation transfer was observed between the 13.46 ppm imino proton of G3 in the neutral pH conformation and the 10.52 ppm imino proton of G3 in the acidic pH conformation. The exchangeable protons at 10.23 and 8.59 ppm are assigned to amino protons at the G3·A10 mismatch in the acidic pH conformation since they exhibit a strong NOE to each other and to imino protons of the flanking G2·C11 and G4·C9 base pairs in the G·A 12-mer duplex at pH 4.2 (Figure 2B).

Nonexchangeable Proton Spectra. The nonexchangeable base and sugar ring protons of the G·A 12-mer duplex have been assigned by analysis of phase-sensitive NOESY spectra (250 and 50 ms mixing times) in D₂O buffer, 25 °C, at pH 6.8 and 4.2. Expanded contour plots of the 250-ms mixing time NOESY spectra establishing distance connectivities between the base protons (7.0–8.6 ppm) and the sugar H1' and cytidine H5 protons (5.0–6.4 ppm) for the G·A 12-mer duplex at pH 6.8 and 4.2 are plotted in Figure 3, parts A and B, respectively. Each base (purine

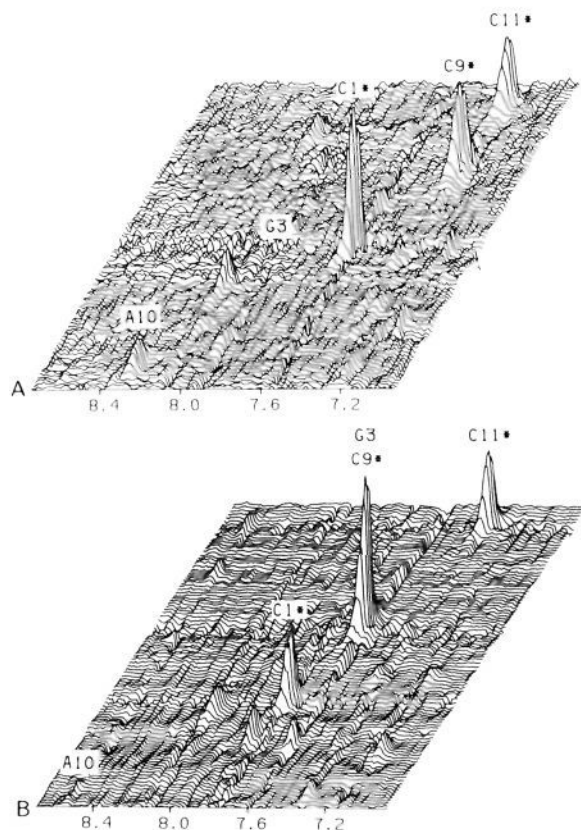


Figure 4. Expanded stacked plots of the phase-sensitive NOESY (50-ms mixing time) spectra of the G-A 12-mer duplex in 0.1 M NaCl, 10 mM phosphate, and D₂O, 25 °C at (A) pH 6.8 and (B) pH 4.2. This region establishes distance connectivities between the base protons (7.0–8.6 ppm) and the sugar H1' and cytidine H5 protons (5.0–6.4 ppm). The cytidine H5–H6 cross peaks are designated by asterisks while the base to its own sugar H1' cross peaks for G3 and A10 are labeled in the figure.

H8 or pyrimidine H6) proton exhibits an NOE to its own and 5'-linked sugar H1' proton²¹ so that the G-A 12-mer sequence can be traced from C1 to G12 including the G3 and A10 residues at the G-A mismatch site for both the neutral pH (Figure 3A) and acidic pH (Figure 3B) spectra.

The strongest cross peaks correspond to the NOEs between the H6 and H5 protons of the cytidines with their short fixed interproton distance of 2.5 Å (designated C1*, C9*, and C11* in Figure 3). The cross-peak intensity of the base to their own sugar H1' NOEs will depend on whether the glycosidic torsion angle is anti (interproton distance 3.7 Å) or syn (interproton distance 2.5 Å). The NOE is weak in the former case and of comparable intensity in the latter case to the NOE between the H6 and H5 protons of cytidine.²² This intensity comparison is best undertaken at short mixing times to avoid artifacts due to spin diffusion. The same expanded regions as in Figure 3 are plotted as stacked plots for the 50-ms mixing time NOESY spectra of the G-A 12-mer duplex in D₂O buffer, 25 °C, at pH 6.8 and 4.2 in Figure 4, parts A and B, respectively. The neutral pH stacked plot demonstrates that the base to its own sugar H1' NOEs for G3 and A10 is much weaker than the NOEs between the H6 and H5 protons of the cytidines (Figure 4A).

The base to sugar H1' NOE for A10 is also weak compared to the NOE between H5 and H6 for the cytidines in the acidic pH stacked plot (Figure 4B). By contrast, the combined cross-peak intensity for the superpositioned NOEs between the base and H1' proton of G3 and between the H5 and H6 protons of C9

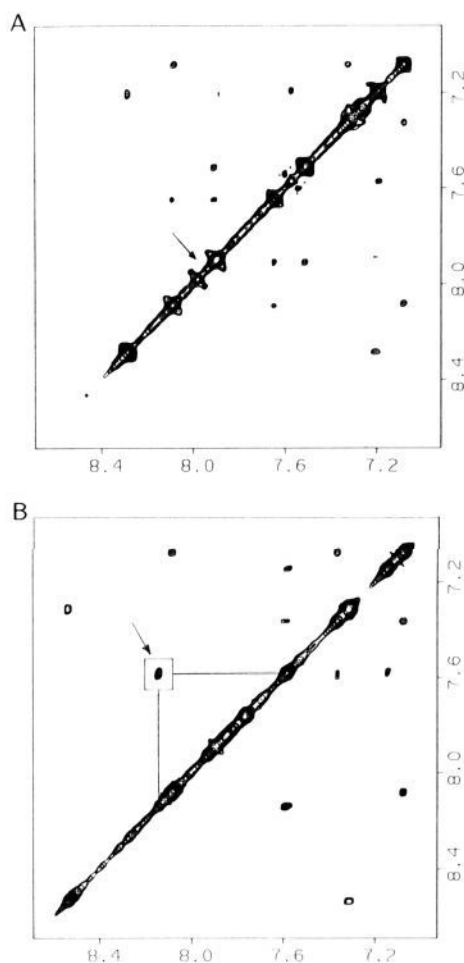


Figure 5. Expanded contour plots of the phase-sensitive NOESY (250-ms mixing time) of the G-A 12-mer duplex in 0.1 M NaCl, 10 mM phosphate, and D₂O, 25 °C at (A) pH 6.8 and (B) pH 4.2. This region establishes distance connectivities between base protons in the symmetrical 7.0–8.4 ppm. The arrow in (A) points out that a cross peak is missing and in (B) that a cross peak is present between the H8 proton of G3 and the H2 proton of A10 at the G3-A10 mismatch site.

(superpositioned cross peaks G3 and C9*, Figure 4B) is twice the intensity for the resolved NOEs between the H5 and H6 protons of C1 and C11 (cross peak C1* and C11*, Figure 4B) in the acidic pH stacked plot.

Expanded NOESY contour plots (250-ms mixing time) of the symmetrical 7.0–8.6 ppm base proton region of the G-A 12-mer duplex in D₂O buffer, 25 °C, at pH 6.8 and 4.2 are plotted in Figure 5, parts A and B, respectively. We detect a cross peak between the H8 proton of G3 and the H2 proton of A10 in the acidic pH contour plot (cross peak designated by arrow, Figure 5B) that is absent in the neutral pH contour plot (designated by arrow, Figure 5A).

A parallel two-dimensional proton NMR study have also been undertaken on the A-G 12-mer duplex (Chart II) at neutral and acidic pH. The exchangeable proton NMR spectra of the A-G 12-mer duplex at acidic pH were broader than the corresponding spectra of the G-A 12-mer duplex at acidic pH. The results for the A-G 12-mer duplex were similar to what were observed for the G-A 12-mer duplex (Figures 1–5) at both neutral and low pH.

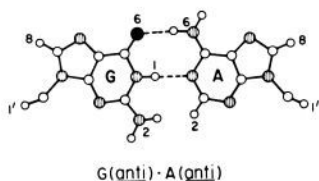
Discussion

The proton NMR data establish that the G-A mismatch in the G-A 12-mer duplex adopts different pairing orientations at neutral pH (pH 6.5–8.5) and at acidic pH (pH 4.0–5.5). (The complete exchangeable and nonexchangeable proton chemical shifts for the G-A 12-mer at neutral and acidic pH are listed in Table II, supplementary material.)

(21) Hare, D. R.; Wemmer, D. E.; Chou, S. H.; Drobny, G.; Reid, B. R. *J. Mol. Biol.* **1983**, *171*, 319–336.

(22) Patel, D. J.; Kozlowski, S. A.; Nordheim, A.; Rich, A. *Proc. Natl. Acad. Sci. U.S.A.* **1982**, *79*, 1413–1417.

Chart III



General Conclusions. The imino proton data (Figures 1, 2) establish formation of stable G2·C11 and G4·C9 Watson-Crick base pairs flanking the G·A mismatch site for the G·A 12-mer at neutral pH (Figure 1A) and at acidic pH (Figure 2A).

The directionality of the base to sugar H1' NOEs (Figure 3) is consistent with formation of right-handed helices²¹ including the segment incorporating the G·A mismatch site in the G·A 12-mer duplex at neutral and acidic pH. Further, the magnitude of the base to sugar H1' NOEs relative to the cytidine H5 to H6 NOEs (Figures 3, 4) demonstrates that the Watson-Crick base pairs adopt anti glycosidic torsion angles²² for the neutral and acidic pH G·A 12-mer duplex conformations.

An NOE is detected between the H8 proton of A10 and the H5 proton of C11 for the G·A 12-mer duplex at pH 6.8 (cross-peak A, Figure 3A) and at pH 4.2 (cross-peak A, Figure 3B). These results establish that A10 adopts a anti orientation about the glycosidic bond at the mismatch site and that the helix is right-handed at the A10·C11 step.

G(anti)·A(anti) Alignment at Neutral pH. Several lines of evidence demonstrate G3(anti)·A10(anti) pair formation (Chart III) for the G·A 12-mer duplex at neutral pH. The magnitudes of the NOEs between the H8 of G3 and its own H1' proton and the H8 proton of A10 and its own H1' proton are both weak compared to the NOEs between the H5 and H6 of cytidines (Figure 4A), consistent with anti glycosidic torsion angles for G3 and A10 at the mismatch site. The observed NOE between the imino proton of G3 and the H2 proton of A10 (Figure 1B) conclusively demonstrates G(anti)·A(anti) pairing (Chart III) for the G·A 12-mer duplex at neutral pH. The anti orientation of the purine-purine bases at the mismatch site increases the cross-strand C1'-C1' separation from its value in purine-pyrimidine pairs. The increased separation may account for the absence of a cross-strand NOE between the H2 proton of A10 in the G3·A10 pair and the H1' proton of G4 in the adjacent G4·C9 pair (Figure 3A) in the G·A 12-mer duplex. The perturbation resulting from the increased C1'-C1' separation also extends to the backbone phosphates as reflected by a 1.5 ppm spectral dispersion for the 11 phosphates in the G·A 12-mer duplex at neutral pH (Figure 6A, supplementary material). One phosphate resonates downfield at 3.22 ppm and another resonates upfield at 4.73 ppm relative to the remaining phosphate resonances that are dispersed between 4.0 and 4.6 ppm for the G·A 12-mer duplex at neutral pH.

The sugar H1' proton of G2 exhibits an unusually high upfield shift of 5.07 ppm (Figure 3A) for the G·A 12-mer duplex at neutral pH suggestive of a perturbation monitored at G2 that is adjacent to the G3(anti)·A10(anti) mismatch site. Similar upfield sugar H1' proton chemical shifts have been previously reported for residue G2 adjacent to the A3·O⁶meG10 O-alkylation site at the dodecanucleotide level²³ and also for a G residue adjacent to the 5'-end of a (A)₅(T)₅ segment of a 11-mer complementary duplex.²⁴ A conformational perturbation is also predicted for the C9·A10 step since the NOE between the H8 of A10 and the sugar H1' of C9 (cross peak designated by arrow, Figure 3A) for the G·A 12-mer duplex at neutral pH was weaker than predicted for an unperturbed helix.

G(syn)·A(anti) Alignment at Acidic pH. The configuration about the glycosidic bond of G3 and A10 defines the pairing orientation at the G3·A10 mismatch site in the G·A 12-mer duplex

Chart IV

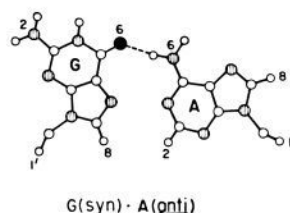
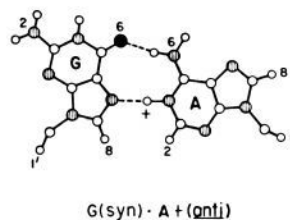


Chart V



at acidic pH. The base to its own sugar H1' NOE for A10 is weak in intensity while that for G3 is comparable in intensity to the NOE between the H5 and H6 protons of cytidine for the acidic pH conformation (Figure 4B). These data demonstrate that G3 is syn and A10 is anti for the G3·A10 mismatch at acidic pH.

The G3(syn)·A10(anti) orientation (Chart IV) is further supported by the observed NOE between the 7.56 ppm H8 proton of G3 and the 8.11 ppm H2 proton of A10 (Figure 5B) for the G·A 12-mer duplex at acidic pH. By contrast, the absence of this NOE is consistent with G3(anti)·A10(anti) orientation (Chart III) for the G·A 12-mer duplex at neutral pH.

The separation between the C1' atoms for a G(syn)·A(anti) mismatch site is comparable to that observed for standard Watson-Crick purine-pyrimidine base pairs. Consequently, the phosphate backbone is minimally perturbed as reflected by an 0.65 ppm spectral dispersion for the 11 phosphates in the G·A 12-mer duplex at acidic pH (Figure 6B, supplementary material).

The formation of a syn orientation at G3 for the G3·A10 mismatch at acidic pH results in an upfield shift of the 5.24 ppm H1' proton of adjacent G4 (cross-peak G4, Figure 3B) along with a perturbation in the C2-G3 step, which results in the NOE between the H8 proton of G3 and the H1' proton of C2 (cross peak designated by arrow, Figure 3B) being weaker than predicted for an unperturbed helix. Further, the cross-strand NOE between the H2 of A10 and the H1' proton of G4 is not detected for the G3(syn)·A10(anti) mismatch site in the G·A 12-mer duplex at acidic pH (Figure 3B).

The imino proton of G3 resonates at 10.52 ppm in the G·A 12-mer duplex at acidic pH (Figure 2A), which corresponds to the chemical shift range for unpaired G imino protons in nucleic acids. The syn orientation of G3 prevents its imino proton from hydrogen bonding with acceptors on A10 and may account for its strandlike value.

We are unable at this time to differentiate definitively between the 2-amino protons of G3 and the 6-amino protons of A10 for the 10.23 and 8.59 ppm amino protons at the G3·A10 mismatch site in the G·A 12-mer duplex at acidic pH (Figure 2A). Both these chemical shifts are ~2 ppm downfield from the 8.0–8.5 ppm and the 6.5–7.0 ppm chemical shifts observed for the hydrogen-bonded and exposed amino protons, respectively. The 2-amino protons of G3 may form hydrogen bonds with the backbone phosphate while the 6-amino proton of A10 forms a hydrogen bond with the 6-carbonyl of G3 in the G3(syn)·A10(anti) orientation (Chart IV).

Protonated G3(syn)·A10(anti) Pair. The observed pH dependence of the conformational transition at the mismatch site may be indicative of protonation of the G(syn)·A(anti) site at acidic pH. The pairing of G3(syn) and A10(anti) would be stabilized by one hydrogen bond in the un-ionized form (Chart IV) and by two hydrogen bonds in the protonated form (Chart V). The trinucleotide segment C9(anti)·A10(anti)·C11(anti)

(23) Patel, D. J.; Shapiro, L.; Kozlowski, S. A.; Gaffney, B. L.; Jones, R. A. *J. Mol. Biol.* **1986**, *188*, 677–692.

(24) Kintanauer, A.; Klevitt, R.; Reid, B. R. *Nucleic Acids Res.* **1987**, *15*, 5845–5862.

Table I. Proton Chemical Shift Differences between the G·A 12-mer Duplex at pH 6.8 (Neutral pH Form) and pH 4.2 (Acidic pH Form)^{a-c}

pair	purine chemical shift differences, ppm						
	NH1	H8	H2	H1'	H2'',2'	H3'	H4'
C1·G12		-0.06		-0.05	-0.02, 0.05	0.0	-0.01
G2·C11	-0.39	0.03		0.79	0.37, 0.02	0.03	0.11
G3·A10	-2.94	-0.34		0.11	-0.35, 0.21	-0.11	-0.07
G3·A10		0.27	0.14	-0.05	0.03, -0.10	0.03	0.04
G4·C9	0.0	0.21		-0.28	-0.07, 0.12	-0.02	-0.06
A5·T8		0.01	-0.07	0.02	-0.02, -0.02	-0.02	-0.02
A6·T7		0.00	-0.02	0.01	-0.01, 0.02	0.0	0.0

pair	pyrimidine chemical shift differences, ppm						
	NH3	H6	H5/CH ₃	H1'	H2'',2'	H3'	H4'
C1·G12		0.25	0.17	0.03	0.13, 0.30	0.04	0.03
G2·C11		0.11	-0.05	0.17	0.17, 0.27	0.10	0.05
G4·C9		0.33	0.29	-0.03	0.31, 0.72	0.08	0.14
A5·T8	0.0	0.04	-0.02	0.06	0.05, 0.07	0.03	0.01
A6·T7	-0.11	0.00	0.0	0.01	0.03, 0.04	0.03	-0.02

^a0.1 M NaCl, 10 mM phosphate, D₂O. ^bPositive chemical shift values reflect acidic pH conformation resonating downfield of neutral pH conformation. ^cExchangeable proton data at 0 °C. Nonexchangeable proton data at 25 °C.

is common to the neutral pH and low pH conformations of the G·A 12-mer duplex. Yet, the H8 proton of A10 resonates at 8.28 ppm in the neutral pH conformation (Figure 3A) and at 8.53 ppm in the acidic pH conformation (Figure 3B) of the G·A 12-mer duplex. This downfield shift at acidic pH may reflect contributions from ring protonation at A10, and hence we favor formation of a G3(syn)·A10+(anti) base pair (Chart V) at acidic pH. The pK_a for adenosine protonation in the free base is approximately 4, but the pK_a for A10 protonation may be much higher when G3(syn)·A10(anti) is embedded in a helix. Similar arguments have been put forward for formation of a protonated A+(anti)·C(anti) base pair.²⁵ We consider G3 protonation of the G3(syn)·A10(anti) pair at acidic pH unlikely since the H8 proton of G3 resonates to high field at acidic pH (7.56 ppm; Figure 3B) compared to neutral pH (7.90 ppm; Figure 3A).

We have not detected an exchangeable resonance that could be assigned to an imino proton between the N1 of A10 and the N7 of G3 corresponding to formation of the second hydrogen bond for the G3(syn)·A10+(anti) mismatch pair (Chart V). Possibly, this could reflect the high exchange rate for this protonated imino proton.

Localized Conformational Perturbation. The chemical shift differences for the base and sugar ring protons of the G·A 12-mer duplex at neutral and acidic pH are listed for the purine and pyrimidine residues in Table I. The largest chemical shift differences are detected in the (G2·G3·G4)·(C9·A10·C11) segment centered about the G3·A10 mismatch site. By contrast, the differences are minimal at the A5·T8 and A6·T7 steps in the center of the helix. These results suggest that insertion of either G3(anti)·A10(anti) or G3(syn)·A10+(anti) pairs results in local conformational perturbations that do not extend beyond the base pairs flanking the purine-purine mismatch site.

The largest nonexchangeable proton chemical shift differences for the G·A 12-mer duplex on proceeding from neutral pH to low pH conformations are downfield shifts of 0.79 ppm for the H1' proton of G2 and 0.72 ppm for the H2' proton of C9 (Table I). These shifts most likely reflect changes in the ring current contributions due to alterations in the stacking patterns at the G3·A10 mismatch site.

Alternate G·A Pairing Schemes. Several pairing orientations have been proposed previously for the G·A mismatch, including the G(anti)·A(anti) pairing^{13,14,16} and the G(anti)·A(syn) pairing,¹⁵ as well as looped out bases at the G·A mismatch site.²⁶

The G(anti)·A(syn) pairing proposed for the G·A mismatch from X-ray studies on a different dodecanucleotide duplex¹⁵ is not supported by our experimental NMR data on either the G·A 12-mer (Chart I) or the A·G 12-mer (Chart II) duplexes.

Further, the present NMR study finds no evidence for G·A mismatch conformations where the bases are looped out of the helix as proposed in a previous NMR study of G·A mismatch containing DNA fragments.²⁶ The NMR studies on G·A mismatches in our paper demonstrate that exchangeable resonances detected between 10 and 11 ppm reflect formation of G(syn)·A+(anti) (Chart V) rather than looping out of the bases at the G·A mismatch site.²⁶

The present experiments have established a pH-dependent equilibrium between G(anti)·A(anti) and G(syn)·A+(anti) pairs for both G·A 12-mer and A·G 12-mer duplexes in aqueous solution. These pairs along with the G(anti)·A(syn) pair establish the presence of more than one type of guanosine-adenosine alignment and may account for the differential recognition of this mismatch by the repair system.

Acknowledgment. We thank Dr. Michael Zagorski, Matthew Kalnik, and Lawrence Shapiro for methodological assistance in the design of the NMR experiments. This research was supported by National Institutes of Health Grant GM-34504. The NMR spectrometers were purchased from funds donated by the Robert Woods Johnson Jr. Trust and the Matheson Trust toward setting up an NMR Center in the Basic Medical Sciences at Columbia University.

Supplementary Material Available: A table of the exchangeable and nonexchangeable proton chemical shifts and a figure of proton-decoupled phosphorus spectra for the G·A 12-mer at neutral and acidic pH (2 pages). Ordering information is given on any current masthead page.

(25) Hunter, W. N.; Brown, T.; Anand, N. N.; Kennard, O. *Nature (London)* **1986**, *320*, 552-555.

(26) Fazakerley, G. V.; Quignard, E.; Woisard, A.; Guschlbauer, W.; van de Marel, G. A. van Boom, J. H.; Jones, M.; Radman, M. *EMBO J.* **1986**, *5*, 3697-3703.